5-2020

Perturbation of Lagrange Points in Effective Potential Simulations

Swapnil Bhatta

The University of Southern Mississippi

Perturbation of Lagrange Points in Effective Potential Simulations

by

Swapnil Bhatta

A Thesis
Submitted to the Honors College of
The University of Southern Mississippi
in Partial Fulfillment
of Honors Requirements

May 2020

Approved by

_____

Michael Vera, Ph.D., Thesis Adviser
Associate Professor of Physics

_____

Bernd Schroeder, Ph.D., Director
School of Mathematics and Natural Sciences

_____

Ellen Weinauer, Ph.D., Dean
Honors College

Abstract

Lagrange points are analytically proven to exist at certain positions in a two-body gravitational system, simply as a function of the gravitational force governing the motion of the bodies and the centrifugal potential due to rotation, providing regions of varying effective potentials. In a system involving interactions between the gravitational forces of multiple bodies however, the position of the Lagrange points ought to change. The purpose of this research project is to verify that the change does indeed occur when a new body is introduced, and compute the perturbation in the position of these points given various parameters.

Keywords: Lagrange points, effective potential.

Acknowledgements

I would like to thank my research adviser, Dr. Michael Vera for his mentorship and encouragement through this project and my academic ventures. I would also like to thank the faculty at the School of Mathematics and Natural Sciences for their support and fostering.

Table of Contents

List of Illustrations vi

Chapter 1: Introduction 1

Rationale 1

Chapter 2: Literature Review 4

Lagrange Points – Analytical Positions 4

Effective Potential 5

Chapter 3: Methodology 7

Computational Approach

Solar System 7

Three-body system 8

N-body system 9

Chapter 4: Results 9

Chapter 5: Conclusion 18

Appendix A: Code 19

Gravitation Potential (gravp.f)

Plots (colorplot.m)

Bibliography 23

List of Illustrations

Figure 1: Lagrange Points. 1

Figure 2: The three-body problem. 3

Figure 3: Combination of effective potential energy. 6

Figure 4: Trojan Asteroids indicating Jupiter's L4. 8

Figure 5: Effective gravitational potential, the Sun and Jupiter. 10

Figure 6: Effective gravitational potential, the Sun, Jupiter and Saturn. 11

Figure 7: Mesh plot of the effective potential. 12

Figure 8: Color plot of the position of L4 and L5. 13

Figure 9-12: Effective potential at various points. 14-17

Chapter 1: Introduction

Lagrange points are points of equilibrium that exist in the vicinity of two orbiting masses. The first three points were discovered by Leonhard Euler in 1765, while the latter two were found by the French-Italian mathematician Joseph Louis Lagrange in 1772. In his publication on the three-body problem, Lagrange discovered a method that considered only the distance between the three bodies rather than their absolute positions [1]. He was able to prove five different configurations in which three bodies can be arranged in such a way that their motion is periodic. The stable points in the configuration were thus named in his honor.

In a two-body non-inertial rotational frame as shown in the figure below, the five equilibrium points are at the given locations indicated by a red circle.

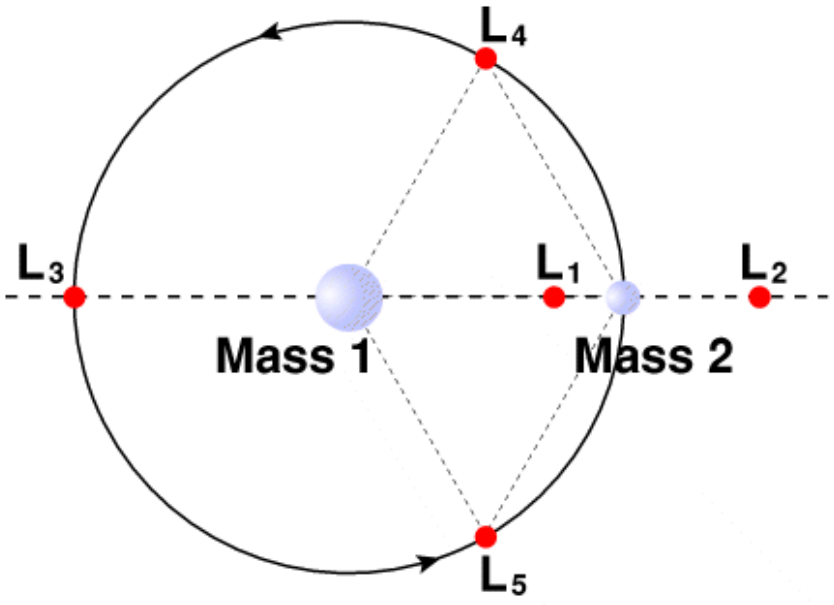

Figure 1: Lagrange Points [2]

a. Rationale:

Lagrange points have applications in space exploration for positioning of satellites, as some of them are pseudo-stable locations at which the effective net force is zero. Thus probes stationed at

such points will be able to maintain their orbits with less positioning required, and thus less fuel consumption. The James Webb Telescope, a satellite that NASA is launching in 2021 will be positioned at the point L2 in the Earth-Sun system. The points are also of interest in cosmology as mass accretion models for binary stars involve these points. A possible interplanetary transport network based on the position of the points is also an aspect of interest [3].

Chapter 2: Literature Review

a. Analytic Positions

The five equilibrium points in the vicinity of two orbiting masses arise analytically due to a solution of the three-body problem. Through assumptions that convert the problem into a restricted three-body problem, and using the equation of motion, various periodic solutions have been obtained by physicists and mathematicians alike.

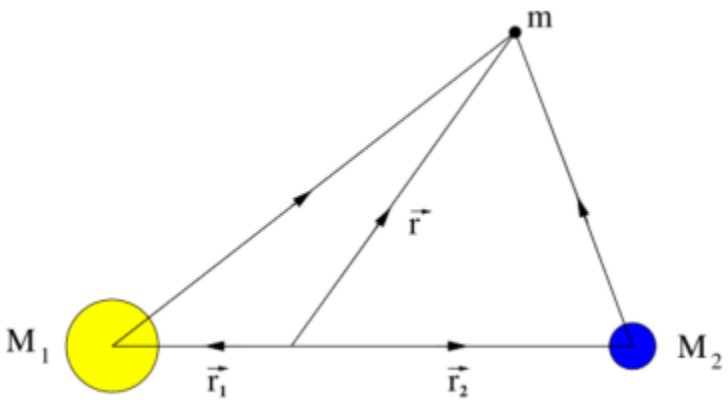

Figure 2: The three-body problem [4]

As shown in the given schematic in Figure 2, given two masses M_1 and M_2, occupying positions of $\mathbf{r_1}$ and $\mathbf{r_2}$, the total force exerted on a third mass m at a position $\mathbf{r}$ is given by;

$$\vec{F} = -\frac{GM_1m}{|\vec{r} - \vec{r_1}|^3}(\vec{r} - \vec{r_1}) - \frac{GM_2m}{|\vec{r} - \vec{r_2}|^3}(\vec{r} - \vec{r_2}) \quad \text{(i)}$$

Using the equation of motion, accounting for a co-rotating frame of reference, the centrifugal force and the Coriolis force, the effective force can be derived from a generalized potential of the following form,

$$U_\Omega = U - \vec{v} \cdot (\vec{\Omega} \times \vec{r}) + \frac{1}{2}(\vec{\Omega} \times \vec{r}) \cdot (\vec{\Omega} \times \vec{r}) \quad \text{(ii)}$$

where Ω is the angular frequency and *U* is the gravitational potential. The second term in the expression is the Coriolis force, and the third term the centrifugal force. Given the Coriolis force is present only in an inertial frame, we assume that it is nonexistent through our solutions. Solving for two-dimensional Cartesian coordinates originating from the center of mass of the system, the points of equilibrium can be analytically found to give the following solutions for the first three points.

$$\begin{aligned} L1: &\quad \left(R\left[1-\left(\frac{\alpha}{3}\right)^{1/3}\right],0\right), \\ L2: &\quad \left(R\left[1+\left(\frac{\alpha}{3}\right)^{1/3}\right],0\right), \\ L3: &\quad \left(-R\left[1+\frac{5}{12}\alpha\right],0\right). \end{aligned} \quad \text{(iii)}$$

where *R*, is the distance between two bodies, α is the mass ratio of the two bodies defined as,

$$\alpha = \frac{M_2}{M_1 + M_2} \quad \text{(iv)}$$

Balancing the radially outward centrifugal force with the gravitational force exerted by the two masses and using appropriate projection vectors one can derive the position of the remaining points, which are equidistant from both bodies. The solution to the last two points in the same coordinate system is given by;

$$\begin{aligned} L4: &\quad \left(\frac{R}{2}\left(\frac{M_1-M_2}{M_1+M_2}\right),\frac{\sqrt{3}}{2}R\right), \\ L5: &\quad \left(\frac{R}{2}\left(\frac{M_1-M_2}{M_1+M_2}\right),-\frac{\sqrt{3}}{2}R\right). \end{aligned} \quad \text{(v)}$$

In terms of positioning of the points in a three-body system, the point L4 and L5 are leading or following the planet's direction of rotation. A look at the shape of an effective potential plot can help determine if the point is at a stable region, based on whether it is at a hill, valley or saddle. Valleys are located in local minimums, making them fairly stable while saddle points are less stable, and hill points unstable. The potential surface will have Lagrange points located in positions where the gradient is zero. Analytically solving the functions for small perturbations in the orbit by linearizing the equation of motion about each solution has shown that L1, L2 and L3 are not stable regions of potential. L4 and L5 however, are stable because of the Coriolis force [5].

b. Effective Potential

The effective potential is a combination of multiple potentials in a system into a single potential. In a non-inertial reference frame for the restricted three body problem, only the gravitational potential energy and the centrifugal potential are incorporated.

The following case illustrates the concept of combined effective potential in the case of the Earth-Moon system with a test mass. The first equation U_{tot} is a combination of the gravitational potential of both bodies along with the centrifugal effect of the rotating reference frame, a version of equation (ii) without the Coriolis force. The second equation is a reduced version of the first equation which shows the paraboloid geometry of the centrifugal component, where μ is the mass ratio, r_1 the distance between the test mass and m_1, and r_2 the distance between the test mass and m_2, l is the angular momentum while x and y are the Cartesian coordinates of the test mass [6]. The given graphs after the equations are potentials plots sliced across an axis for better visual representation.

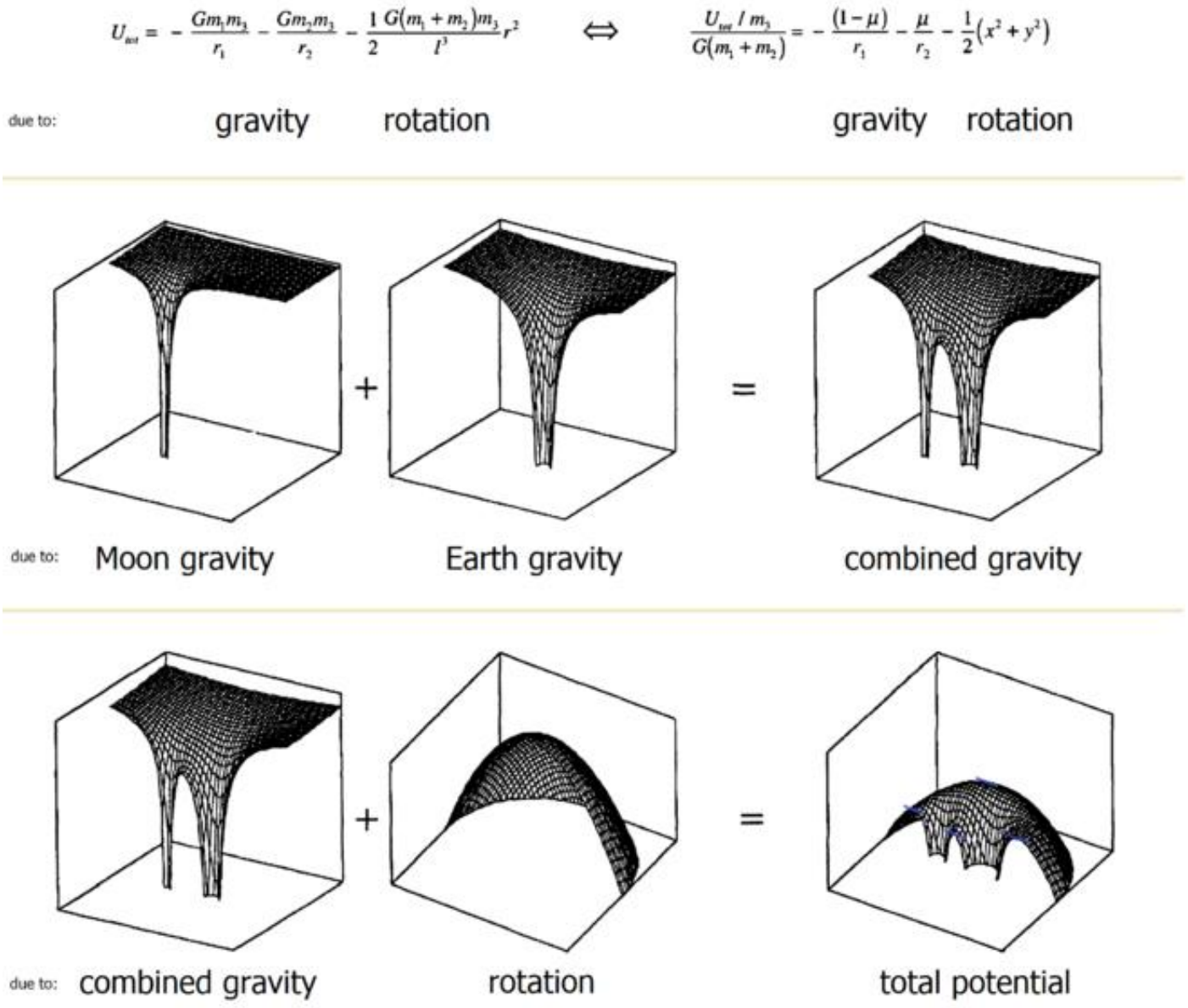

Figure 3: Combination of effective potential energy, as shown in [6].

Chapter 3: Methodology

a) Computational Approach

The computational portion of the project was built off of previous work done on the influence of other heavenly bodies on satellite positioning [7]. Data from NASA's New Horizons program was used to obtain positioning of various celestial bodies in our solar system. The current project was initially geared toward determining the perturbations based on the positioning of live space missions and the position and mass parameters of Earth and nearby planets. The computations based on this proved to be challenging as the mass of the Sun, a colossal 1.989×10^{30} kg dwarfed the potential values for all planets except for the outer gas giants. The approach was then shifted to observe the position of the points and see if changes in potential values were encountered when simulating systems with effective potential values that could be turned into something tangible. Celestial systems as the ones used for the computations do exist in the form of binary star systems or circumbinary planet systems but are rare. The color plots and the mesh plots generated based on the effective potential values of these systems were very helpful in visualizing the changes, while numerical analysis was used to measure these changes.

The computational approach focused on the points L4 and L5, as these are the most interesting given the extended stability.

i.Solar System:

The actual parameters of the gas giants, Jupiter and Saturn, were used to calculate the effective potential for Jupiter's L4 and L5 Lagrange points, home to the famous Trojan Asteroids. The gravitational potential for Saturn was then added and the effective potential values were checked for possible changes to the position of the points.

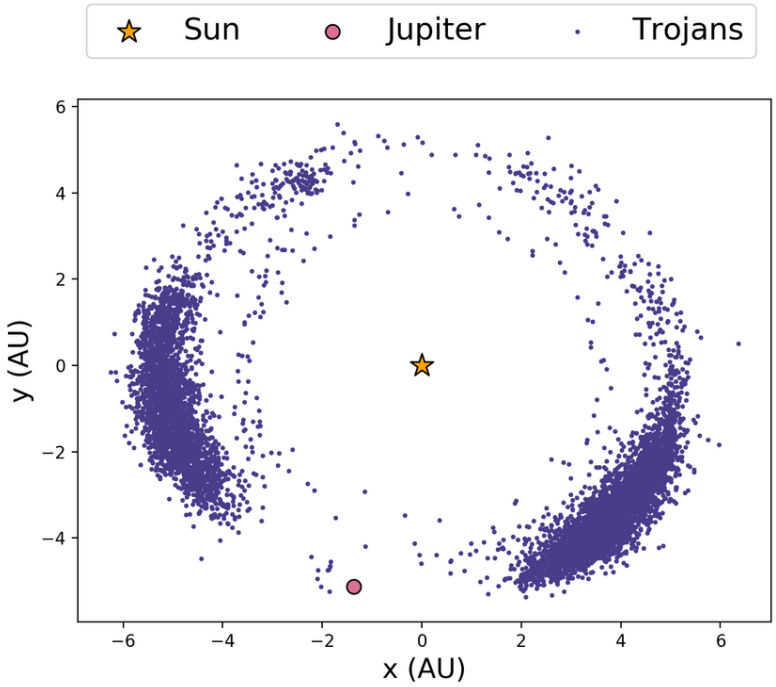

Figure 4: Trojan Asteroids indicating Jupiter's L4 (group on the left) and L5 point (group on the right), from [8].

ii.Three-body system

A three-body system was created with a massive body at the center of our coordinate system, with a given mass of 99. It was orbited by a smaller body of mass 1 at a radius of 1. The value for the gravitational constant was treated as being 1. The third body in this case is simply a test mass, and we proceed with the assumption that it does not have a gravitational field of its own. The center of mass was firstly computed and factored into the potential formula to get a better value for the separation distance. The derived formulas for the position of the Lagrange points in equations (iv) and (v) assumed the position of the smaller body to be along the x-axis, therefore a rotational matrix was factored into the potential formula to account for different positions.

iii.n-body system

Once the expected positions for the Lagrange points were verified for a three-body system, the code for the effective potential was adjusted to factor in the gravitational potential from other bodies. The new bodies had a position that could be rotated, while maintaining the initial position of the first two bodies by assuming a co-rotating frame with respect to the first two bodies. The maximum value for the effective potential was then determined, which was the coinciding position of the points depending on whether the point is following or leading the planet in its motion. A lot of other bodies could in theory be incorporated as the assumption was a non-inertial frame, however stable configurations of such mass ratios are rare in the cosmos and addition of more masses could push the study into more hypothetical systems than physically plausible ones. The plots also have the position of the bodies denoted, but these are not to scale.

Chapter 4: Results:

i. Solar System

The following table lists the initial values for the Sun, Jupiter and Saturn acquired from the New Horizons program, based on the positions of the entities on April 27, 2012 [9].

Object	X (AU)	Y (AU)	Mass (kg)
Sun	0	0	1.9891×10^{30}
Jupiter	0.7719208023413598	-5.15967904259965	1.8986×10^{27}
Saturn	-8.487285193590072	3.763807729501108	5.6846×10^{26}

Table 1: Initial Conditions

The following plot in Figure 6 depicts the effective potential that results when only Jupiter and Sun are considered as a two-body system.

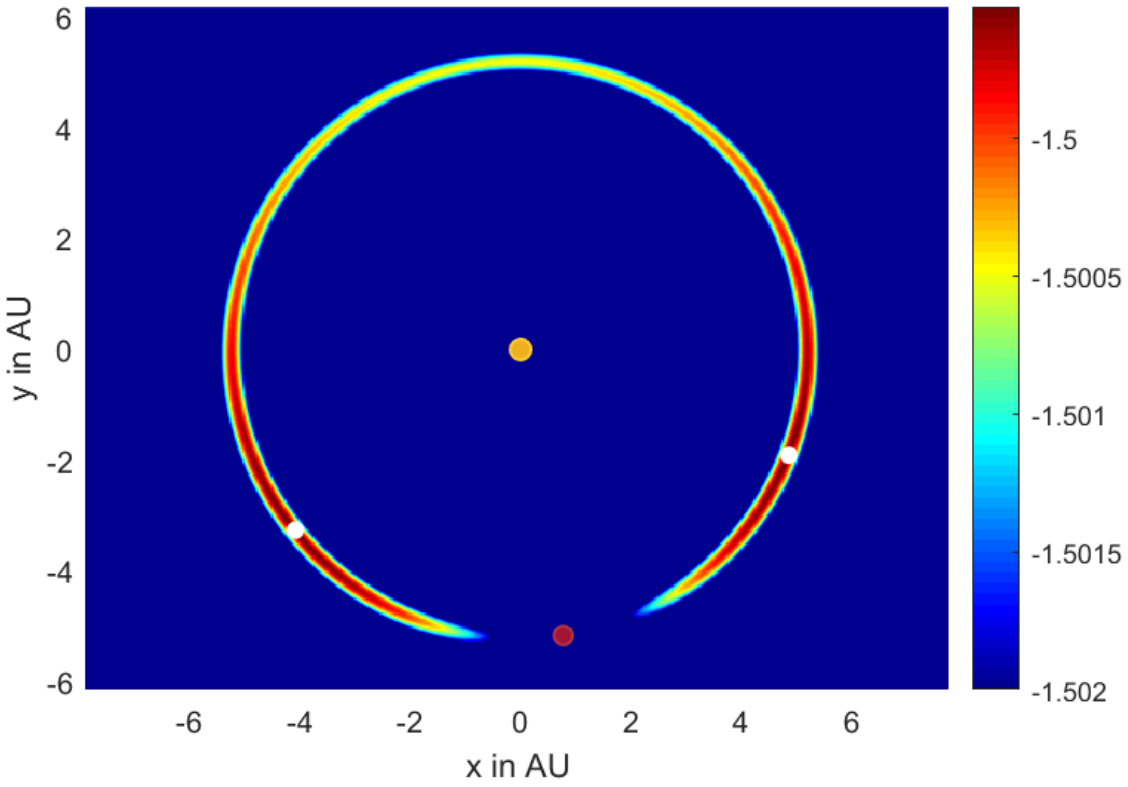

Figure 5: The effective gravitational potential is shown with L4 and L5 (white), the Sun (yellow) and Jupiter (red).

Lagrange Point	X (AU)	Y (AU)
L4	4.85363888	-1.90641688
L5	-4.08319003	-3.24342333

Table 2: Position of the points.

When Saturn is included in the computation, the effective potential field is distorted as can be seen in Figure 7. It may not be visible that the points have shifted, though some asymmetry in the potential field is evident. The determination of the position of the maximum effective potential indicated a change had indeed occurred in the location of the points.

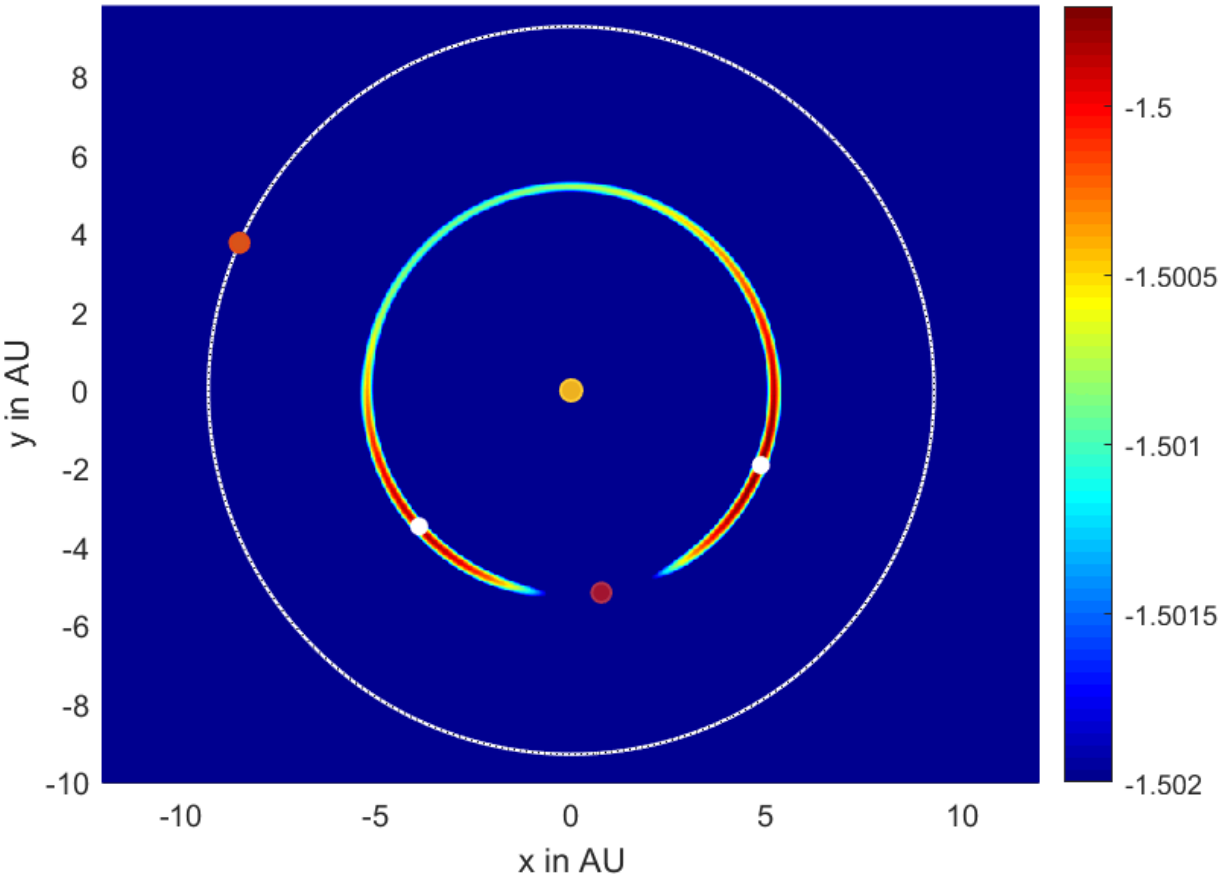

Figure 6: The effective gravitational potential is shown with L4 and L5 (white), the Sun (yellow), Jupiter (red) and Saturn (Orange).

Changed Lagrange Point	X (AU)	Y (AU)
L4	4.8511	-1.9074
L5	-3.8899	-3.4693
Magnitude of Deviation:	0.00272258	0.29729

Table 3: Changed position of the points.

ii. N-body

The first simulation utilized the following parameters

Object	X (AU)	Y (AU)	Mass
M1	0	0	99
M2	1	0	1

Table 4: Initial Conditions

This two body test system was developed for a mass ratio of 99:1. While not as dominant as the actual solar mass, the size of the central mass enables the center of mass for the system to be approximated by its location.

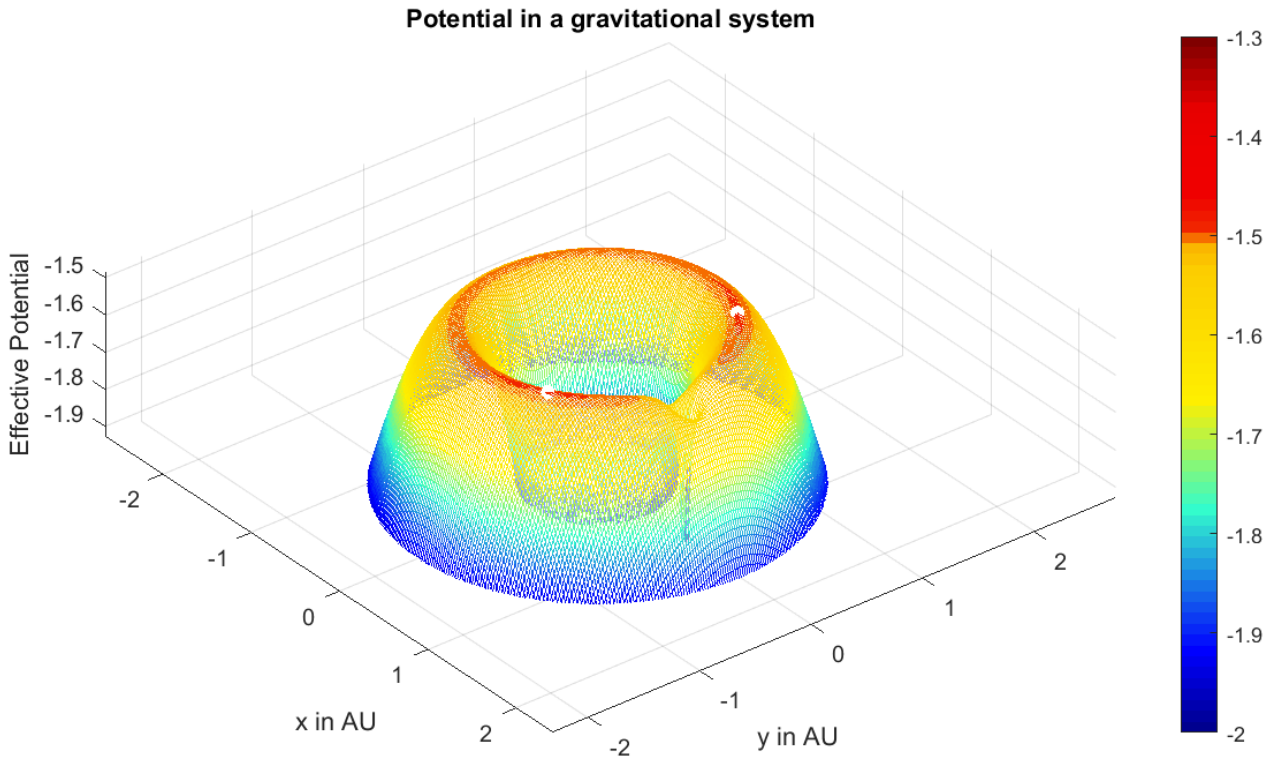

Figure 7: Mesh plot of the effective potential, with the L4 and L5 points shown in white.

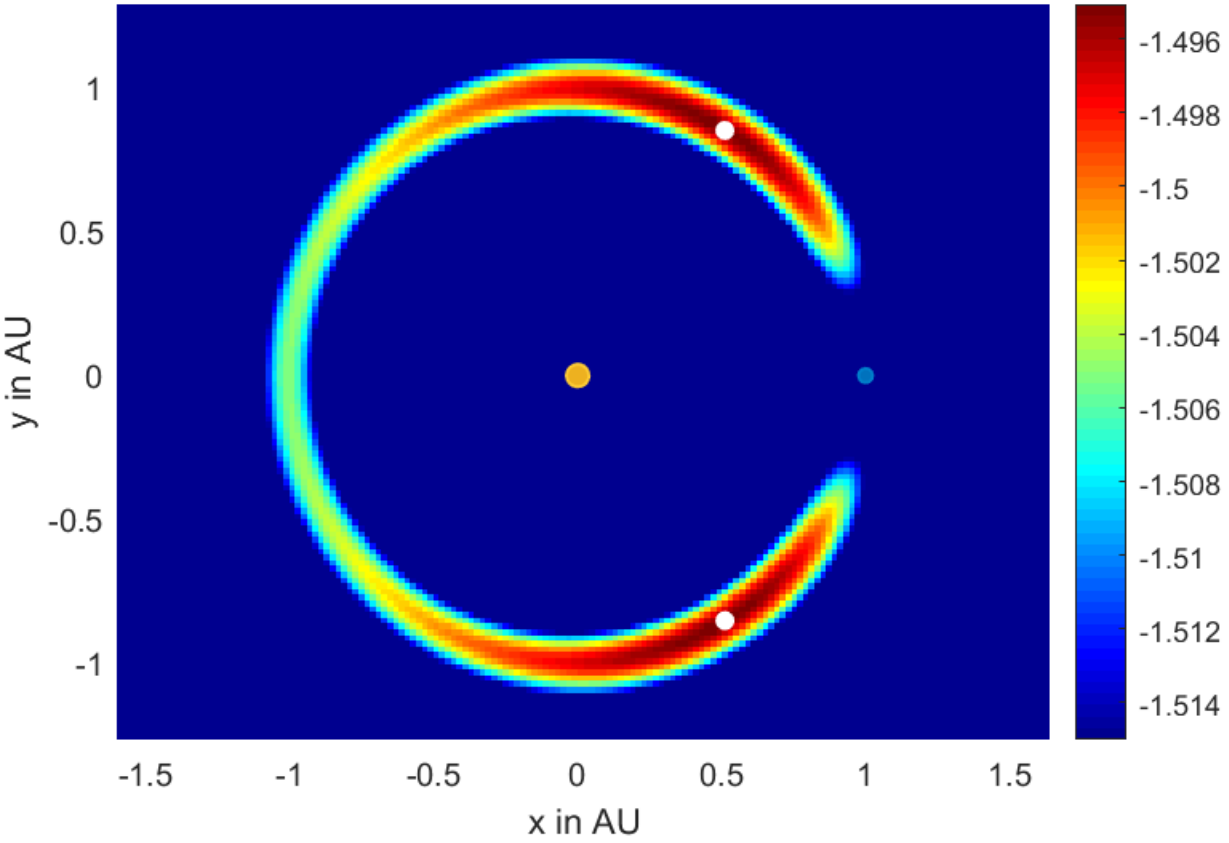

Figure 8: Color plot of the position of L4 and L5.

Lagrange Point	X (AU)	Y (AU)
L4	0.49	0.866025388
L5	0.49	-0.866025388

Table 5: Position of the points.

The effective potential field depicted in the previous section was then reassessed after the introduction of a third body. This body, denoted as M3, had a mass of 2 (in units where the central body has a mass of 99 and the original orbiting body has a mass of 1). The body of mass 2 was placed at a radius from the central body that is triple that of the original orbiting body.

a) M3 at (3,0)

In this simulation, the object M3 is along the x-axis at coordinates (3,0).

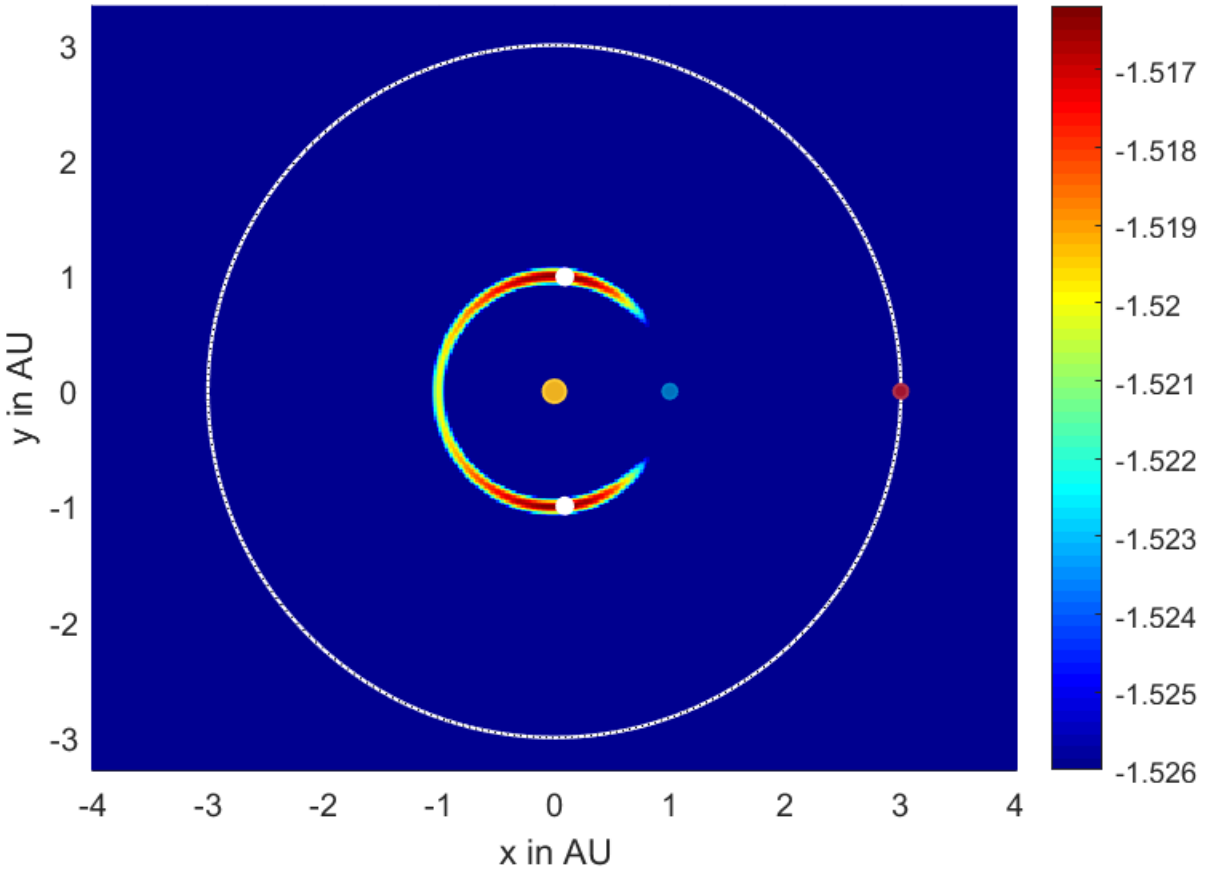

Figure 9: The effective gravitational potential is shown with L4 and L5 (white), M1 (yellow), M2 (blue) and M3 (Red).

Changed Lagrange Point	X (AU)	Y (AU)
L4	0.0902	0.9925
L5	0.0902	-0.9925

Table 6: Changed position of the points.

	L4 (AU)	L5 (AU)
Magnitude of Deviation:	0.419328	: 0.419328

Table 7: Magnitude of Deviation.

b) M3 at (3/√2, 3/√2)

In this simulation, the object M3 has rotated by 45 degrees and is now at (3/√2, 3/√2)).

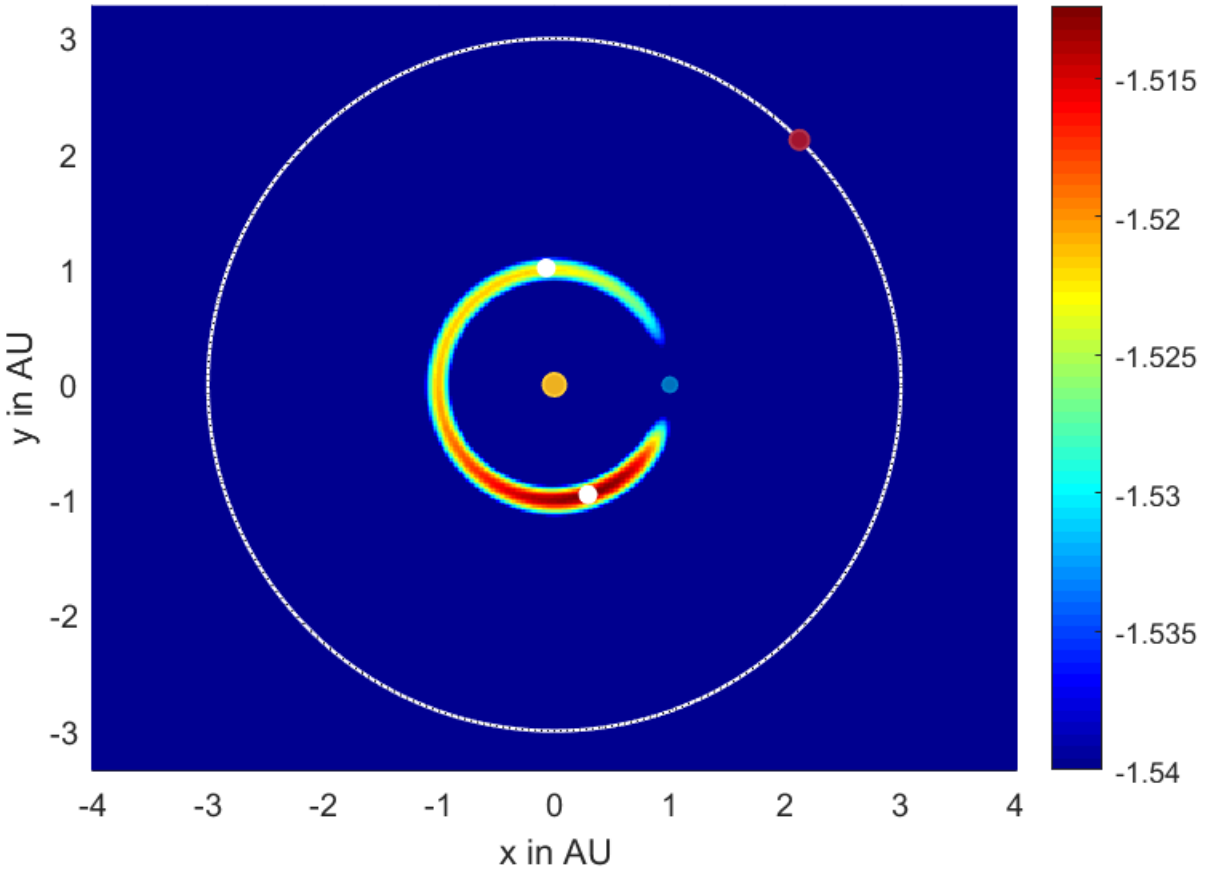

Figure 10: The effective gravitational potential is shown with L4 and L5 (white), M1 (yellow), M2 (blue) and M3 (Red).

Changed Lagrange Point	X (AU)	Y (AU)
L4	-0.0702	1.0125
L5	0.2907	-0.9524

Table 8: Changed position of the points.

	L4 (AU)	L5 (AU)
Magnitude of Deviation:	0.579033	0.217212

Table 9: Magnitude of Deviation.

c) M3 at (0, 3)

In this simulation, the object M3 has rotated by 90 degrees and is now at (0, 3).

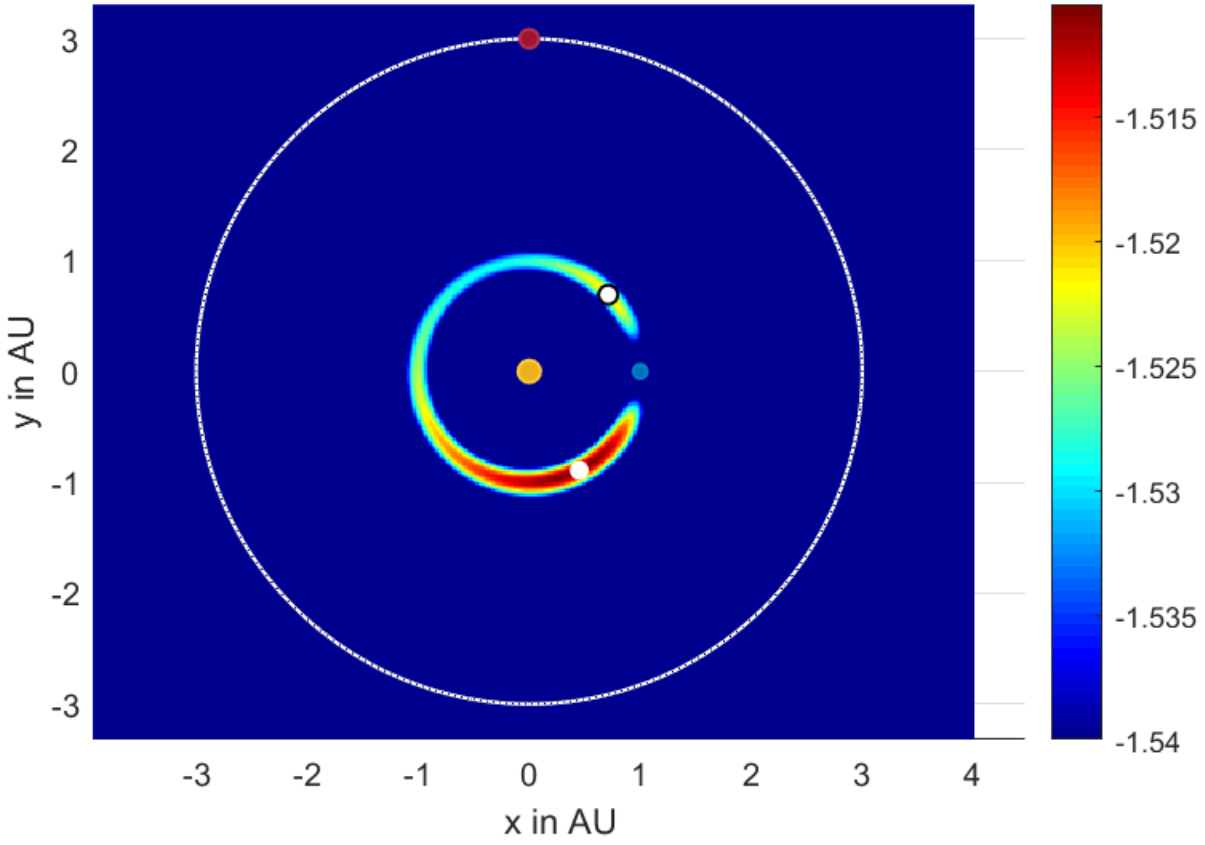

Figure 11: The effective gravitational potential is shown with L4 and L5 (white), M1 (yellow), M2 (blue) and M3 (Red).

Changed Lagrange Point	X (AU)	Y (AU)
L4	0.7118	0.6917
L5	0.4511	-0.8922

Table 10: Changed position of the points.

	L4 (AU)	L5 (AU)
Magnitude of Deviation:	0.282107	0.0468862

Table 11: Magnitude of Deviation.

d) M3 at (-3/√2, -3/√2)

In this simulation, the object M3 has rotated by 225 degrees and is now at (-3/√2, -3/√2)).

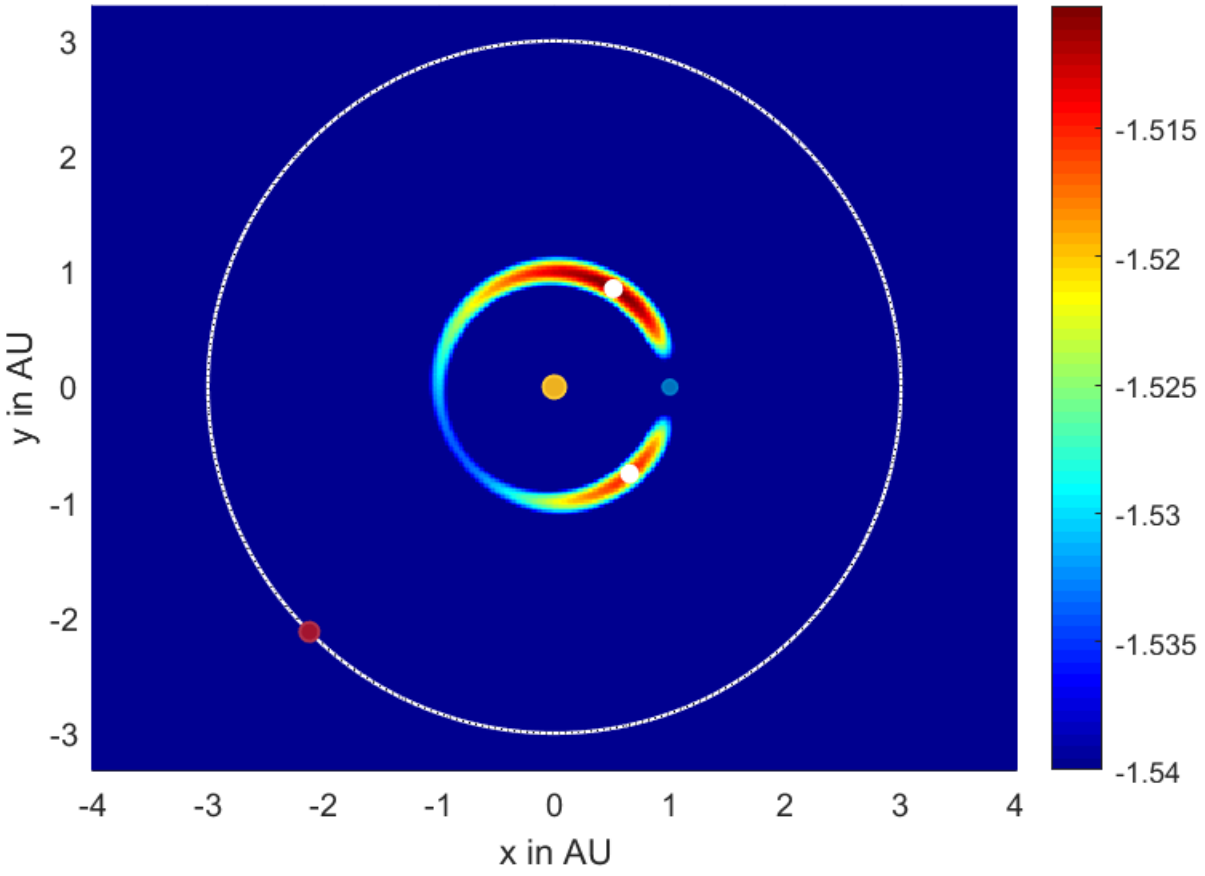

Figure 12: The effective gravitational potential is shown with L4 and L5 (white), M1 (yellow), M2 (blue) and M3 (Red).

Changed Lagrange Point	X (AU)	Y (AU)
L4	0.5113	0.8521
L5	0.6516	-0.7519

Table 12: Changed position of the points.

	L4 (AU)	L5 (AU)
Magnitude of Deviation:	0.0254481	0.197836

Table 13: Magnitude of Deviation.

Chapter 5: Conclusions

There were visible perturbations in the Lagrange points L4 and L5 in all scenarios where additional gravitational potentials were introduced. For the test involving actual astronomical parameters, Saturn was added to the two-body system of the Sun and Jupiter. Location perturbations of Lagrange points with magnitude 0.00272258 (L4) and 0.29729 (L5) were identified. In the model system, magnitudes ranging from a mere 0.0468862 [L5, M3 at (0,3] to a rather significant 0.579033 [L4, M3 at ($3/\sqrt{2}$, $3/\sqrt{2}$)] were identified. The magnitude of the difference was relatively low for the astronomical parameters. This is mostly due to the dominance of the Sun's gravitational potential. When the mass ratios were not as extreme, the difference in positions was quite significant, enough to completely change the location of any potential equilibrium for an object intended for the Lagrange point.

One issue that could be better addressed in future explorations of the topic would be to account for the change in the center of mass due additional bodies. Similar test systems could be utilized in dynamical simulations in which the positions of the involved bodies are updated using gravitational forces and appropriate numerical methods for advancing differential equations [10]. Effective potential tests in different dynamic systems that have known stable configurations, such as the previously mentioned circumbinary orbit or a figure eight orbit would also be potential future projects of interest.

Appendix A: Code

FORTRAN file gravp.f

```
subroutine gravp(nbod,v,rpt,r,m,potl)
      implicit double precision(a-h,o-z),integer(i-n)
      double precision rpt(3),r(10,3),m(10)
c G in AU,day from original ss.f code via wikipedia on G
      g=1.488180714e-34

c a= the distance between two bodies
      a=sqrt((r(1,1)-r(2,1))**2+(r(1,2)-r(2,2))**2)
      cosiv=r(2,1)/(sqrt(r(2,1)**2+r(2,2)**2))
      sinev=r(2,2)/(sqrt(r(2,1)**2+r(2,2)**2))
c om=Reduced Mass Ratio
      om=m(1)/(m(1)+m(2))
c compute potential of the body at the center.
      term2=-om/sqrt((rpt(1)/a+cosiv*(1-om))**2+(rpt(2)/a+sinev*(1-om))**2)
c centrifugal potential due to only earth and sun
      term3=-0.5*(((rpt(1)**2)/a**2)+((rpt(2)**2)/a**2))
      potl=0
      do 110 inb=2, nbod
        cosiv=r(inb,1)/(sqrt(r(inb,1)**2+r(inb,2)**2))
        sinev=r(inb,2)/(sqrt(r(inb,1)**2+r(inb,2)**2))
        a=sqrt((r(1,1)-r(inb,1))**2+(r(1,2)-r(inb,2))**2)
c om=Reduced Mass Ratio
        om=m(1)/(m(1)+m(inb))
c compute m2/abs(r-r1)
        term1=(-1+om)/sqrt((rpt(1)/a-cosiv*om)**2+(rpt(2)/a-sinev*om)**2)
        potl=potl+term1
 110  continue
      potl=potl+term2+term3
      return
      end
```

MATLAB colorplot.m

```
dat = load('outputs/outse');

[height, length] = size(dat);
%Finding the intervals
dx=dat(((height)^.5+1),1)-dat(1,1);
```

```
dy=dat(2,2)-dat(1,2);

%creating a vector x with all the needed divisions
x=[dat(1,1):dx:dat((height),1)];
%Fixing the floating-point arithmetic issue of 1x399
x=[x,dat(height,1)];

%same with y
y=[dat(1,2):dy:dat(sqrt(height),2)];
y=[y,dat(sqrt(height),2)];

%create a new matrix to have values for potential
potl=zeros(sqrt(height),sqrt(height));
for ix=1:sqrt(height);
        for iy=1:sqrt(height);
            potl(ix,iy)=dat(sqrt(height)*(ix-1)+iy, 3);
        end
end

%Mesh & Contour plot
figure
mesh (x, y, potl','FaceAlpha','0.5')
xlabel('x in AU')
ylabel('y in AU')
zlabel('Effective Potential')
title('Potential in a gravitational system')
axis tight
colorbar
zlim([-3 max(max(potl))])
colormap(jet)    % change color map

maximum = max(max(potl));
[px,py]=find(potl==maximum)

figure
hold on
imagesc(x,y',potl',[-1.6 max(max(potl))])
xlabel('x in AU')
ylabel('y in AU')
```

```
grid on
axis('equal')
set(gca,'YDir','normal')
colormap('Jet')

%Plotting maximum point/points
for i=1:size(px)
    scatter(x(px(i)), y(py(i)),'w','filled')
end

% potlex=potl;
% potlex(:,1:200)=-100;
% maximum = max(max(potlex));
% [px,py]=find(potlex==maximum)
% x(px)
% y(py)

%scatter(x(px), y(py),'MarkerEdgeColor',[0 0
0],'MarkerFaceColor',[1 1 1],'LineWidth',1)

%Orbit as needed
viscircles([0 0],3,'LineStyle',':', 'Color', 'k',
'LineWidth', 0.1)

%PLotting the position of the planets/sun
%Jupiter
scatter(7.719208023413598E-01,-5.159679042599656, 40,
'MarkerEdgeColor',[0.7 0.2
0.3],'MarkerFaceColor',[0.6350 0.0780
0.1840],'LineWidth',1)
%Saturn
scatter(-8.487285193590072E+00,3.763807729501108, 40,
'MarkerEdgeColor',[0.9 0.3
0.09],'MarkerFaceColor',[0.8500 0.3250
0.0980],'LineWidth',1)
%Sun/M1
scatter(0, 0, 50,'MarkerEdgeColor',[1 0.8
0.2],'MarkerFaceColor',[0.9290 0.6940
0.1250],'LineWidth',1)
```

```
%"M2"
scatter(1, 0, 20,'MarkerEdgeColor',[0 0.5
0.8],'MarkerFaceColor',[0 0.4470 0.7410],'LineWidth',1)
%"M3"
scatter(0, 3,'MarkerEdgeColor',[0.7 0.2
0.3],'MarkerFaceColor',[0.6350 0.0780
0.1840],'LineWidth',1)

hold off;
```

Bibliography

[1] Joseph Lagrange. LE PROBL'EME DES TROIS CORPS. 1772. https://gallica.bnf.fr/ark:/12148/bpt6k229225j/f231. Accessed April 2020.

[2] Image: Lagrange Points, https://simple.wikipedia.org/wiki/Lagrange_point#/media/File:Lagrange_2_mass.gif, Accessed April 2020.

[3] Shane D. Ross, The Interplanetary Transport Network, 2006, http://www.dept.aoe.vt.edu/~sdross/papers/AmericanScientist2006.pdf, Accessed April 2020.

[4] Neil J. Cornish, WMAP Education Outreach - Lagrange Points, 1998, https://map.gsfc.nasa.gov/ContentMedia/lagrange.pdf, Accessed April 2020.

[5] Thomas Greenspan, Stability of Lagrange points, L4 and L5, 2014, http://pi.math.cornell.edu/~templier/junior/final_paper/Thomas_Greenspan-Stability_of_Lagrange_points.pdf, Accessed April 2020.

[6] Image: Energy Potential Analysis, https://en.wikipedia.org/wiki/File:Restricted_Three-Body_Problem_-_Energy_Potential_Analysis.png, Accessed April 2020.

[7] Aaron J. Wise, "An Analysis of Satellite Orbit Perturbations", Physics Thesis, Univ. Southern Miss. (2012).

[8] Malena Rice, "Distribution of all modeled Jovian Trojan asteroids", https://www.researchgate.net/publication/333160345_The_Case_for_a_Large-Scale_Occultation_Network/figures?lo=1&utm_source=google&utm_medium=organic, Accessed April 2020.

[9] HORIZONS System. https://ssd.jpl.nasa.gov/?horizons, Accessed March 2019.

[10] Michael Vera, Computational Methods for Physical Systems II (University of Southern Mississippi, 2010).